# Effect of annealing on structural and optical properties of ZnS nanocrystals

G. MURALI[a], D. AMARANATHA REDDY[a], B. POORNAPRAKASH[a], R. P. VIJAYALAKSHMI[a*], N. MADHUSUDHANA RAO[b]
[a]*Department of Physics, Sri Venkateswara University, Tirupati-517502, India*
[b]*School of Advanced Sciences, VIT University, Vellore-632 014, India*

ZnS nanocrystals (NCs) (~2.66 nm) capped with 2-mercaptoethonal were synthesized from $Na_2S$ and Zinc acetate using a chemical co-precipitation method. Structural, morphological and optical properties of ZnS NCs annealed in air at temperatures up to 600 $^0$C are presented. High temperature wurtzite phase of ZnS appeared at 400 $^0$C and annealing up to 600 $^0$C results in change of compound from ZnS to ZnO. Agglomeration of particles increased with increasing annealing temperature was observed from scanning electron microscopy (SEM) images. Decreasing of band gap with increasing annealing temperature was observed from diffuse reflectance studies (DRS) studies. Temperature dependent quenching and raising behavior of photoluminescence (PL) emissions accompanied by a red shift of PL peak from violet region to green region was observed.

(Received August 18, 2011; accepted September 15, 2011)

*Keywords*: Nanocrystals, ZnS, Annealing, Redshift

## 1. Introduction

Nanoscale materials are of considerable interest due to their peculiar and fascinating properties and applications superior to their bulk counterparts [1-3]. Nanoparticles often referred to as artificial atoms, are predicted to have discrete, atomic like energy levels and a spectrum of ultra-narrow transitions that is tunable with size of quantum dot [4-7]. Hence, compared with bulk materials, nanocrystals exhibit distinct electronic, optical, chemical and thermal properties as a result of large surface areas and quantum confinement effects. A variety of synthetic methods exist for controlling the size, shape and composition of the nanoparticles, allowing for the tailoring of properties specific to desired application. In solution based chemical method, a capping agent, which adsorbs to the nanocrystal surface, is generally added in order to control the size of the particle and to prevent agglomeration. These absorbates have been shown to alter the electronic structure of the nanocrystals [8, 9].

ZnS an important semiconductor compound of the II-VI group has attracted great attention with excellent physical properties and wide band-gap energy of 3.68 eV [10] at room temperature. There exists two basic structures of bulk ZnS, one is the cubic Zinc-blende structure and the other one is the hexagonal wurtzite structure. The cubic (Zinc blende) form of ZnS is stable at room temperature, while wurtzite, the less dense hexagonal form is stable at above 1020 $^0$C [11, 12]. ZnS is also well-known phosphor material with various luminescent properties, such as photoluminescence (PL) and electroluminescence (EL). It has been extensively investigated for variety applications in various fields such as photonic crystal devices operating in the region from visible to near IR, nonlinear optical devices, displays, sensors, infrared Windows and lasers [13 - 17]. Owing to its large band gap (3.68 eV), ZnS absorbs only in the UV. However, its absorbance and photoluminescence can be easily tuned by doping with transition metal ions [18-21] and by heat treatments [22, 23].

Annealing treatments are very common in semiconductor processing. The annealing can be used to improve the crystal quality and to confirm the stability of the crystal at a given temperature, which is important for device purposes. An annealing treatment is quite effective for reproducible size control of ZnS NCs [24]. To the best of our knowledge there are only few reports on the annealing effects on ZnS NCs. In view of this, in the present work, we report the influence of thermal annealing in air on the structural and optical properties of ZnS NCs, which are prepared using chemical co-precipitation method.

## 2. Experimental

ZnS nanoparticles were synthesized using a chemical co-precipitation method at room temperature. All the chemicals which are used as source materials i.e zinc acetate and sodium sulphide are of AR grade (Merck and SD fine chemicals) and used without further purification. Appropriate quantities of these were weighed according to the stoichiometry and were dissolved in distilled water to make 0.2 M solutions. The aqueous solution of $Na_2S$ was mixed under continuous stirring using magnetic stirrer with solution containing zinc acetate. An appropriate amount of 2-mercaptoethonal (0.5 ml) was also added to the reaction medium to stabilize the particle surfaces. After complete precipitation, the solution in conical flask was stirred for about 8 hours. The final product was filtered out and washed with de-ionized water several times and then dried at 80 $^o$C for 10 h, to remove both water and organic capping agent and other by products formed during the reaction process. The dried flakes were crushed in a pestle-motor till very fine powder was

obtained. These powders were air annealed at 300, 400, 500 and 600 $^0$C for 2 h and collected in airtight containers and then used for all measurements.

To determine the structure of the ZnS host and the sizes of the crystallites before and after annealing, X-ray diffraction studies were carried out using a Seifert 3003 TT X-ray diffractometer with Cu-Ka radiation with a wavelength of 1.542 Å. Diffraction patterns were recorded over a range of 20 - 80$^o$. Chemical analysis and morphological studies were carried out using scanning electron microscopy (SEM) with EDAX attachment (model CARL-ZEISS EVO MA 15). Photoluminescence (PL) measurements were carried out at room temperature using OBIN YOUN Fluorolog-3 spectrometer with a 450W Xenon arc lamp as an excitation source. Diffuse reflectance spectra of the samples were recorded at room temperature using Jasco V 570 UV-Vis spectrophotometer in the wavelength range 200–460 nm.

## 3. Results and discussion

The compositional analysis of ZnS NCs was performed by EDAX analysis. Three EDAX spectra representatives of the ZnS (as synthesized, annealed at 300 and 600 $^0$C) are shown in Fig. 1. In as synthesized ZnS, elemental Zn and S were found in a near stoichiometric ratio. The variation in the relative intensity of O line with respect to S line for annealing temperatures (300 and 600 $^0$C) is clearly evident from Fig. 1. The observed variations are due to the oxidation of sulfur during the annealing process.

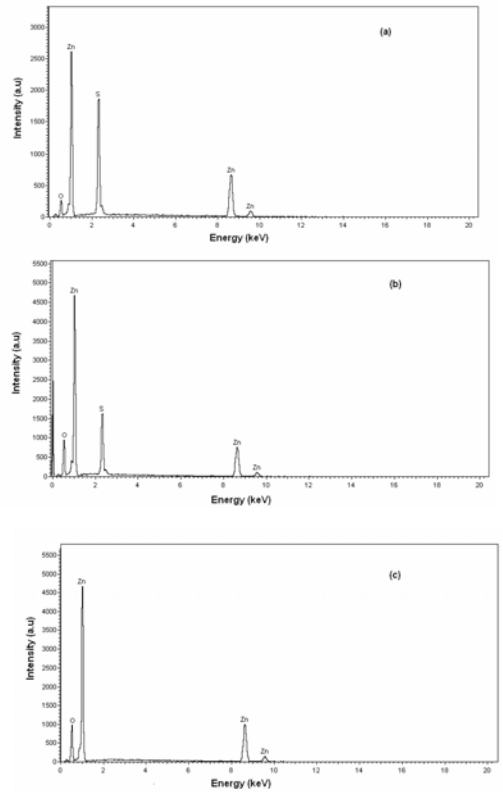


*Fig. 1. EDAX spectra of ZnS NCs: Spectra for as synthesized (a) and annealing at 300 $^0$C (b) at 600 $^0$C (c).*

The XRD spectra of ZnS NCs before and after annealing at various temperatures are shown in Fig. 2. Change in phase, crystallinity and orientation are clearly evident from these spectra by increasing the annealing temperature. From the figure it is evident that all the diffraction peaks from the as synthesized nanocrystals are very broad, but matched the Bragg angels measured for bulk ZnS (111), (220) and (331) of the cubic phase. This indicates the absence of impurities in the prepared sample. It is known that decrease in particle size results in a broadening of the diffraction peak.

A faint proportion of wurtzite structure was appeared in the sample annealed at 400 $^0$C. The weight of wurtzite in the mixture increases with increasing temperature, and it become rather dominant for the sample annealed at 500 $^0$C. From Fig. 2, it is clearly evident that the wurtzite peaks (100) and (101) are clearly visible next to the zinc blende peak (111). In addition, the presence of three peaks at angles ~31$^0$, ~34$^0$ and ~36$^0$ for the samples annealed at 500 $^0$C depicts the formation of wurtzite ZnO along with predominant wurtzite ZnS. However, ZnS phase almost disappears and ZnO phase appeared when the annealing temperature increased from 500 $^0$C to 600 $^0$C.

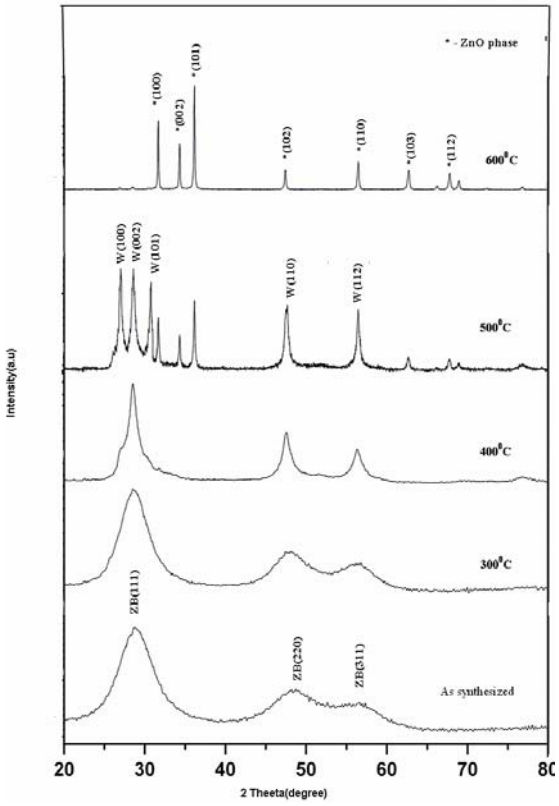


*Fig. 2. XRD spectra of as synthesized and annealed ZnS NCs.*

The average crystallite size is calculated from the full-width at half-maximum (FWHM) of the most intense diffraction peaks using the Debye-Scherrer formula:

$$D=0.89\,\lambda / \beta \cos\theta$$

Where, D is the mean crystallite size, $\lambda$ the X-ray wavelength, $\beta$ the FWHM of the diffraction peak and θ the diffraction angle. The mean crystallilte sizes of subcrystal before annealing was 2.66 nm and it was observed that the particle size increased with increasing annealing temperature. Such a variation in particle size is clearly evident from Fig. 2 that the broadening of the diffraction peaks decreased with increase in annealing temperature. The size of the NCs annealed at 500 $^0$C is calculated to be 34.6 nm, which was almost agreement with the values estimated from the TEM image shown in Fig. 3.

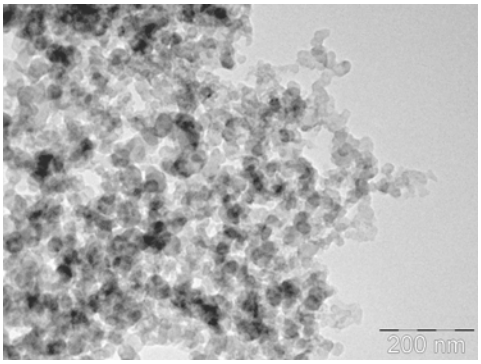


*Fig. 3. TEM of ZnS nanoparticles annealed at 500 $^0$C.*

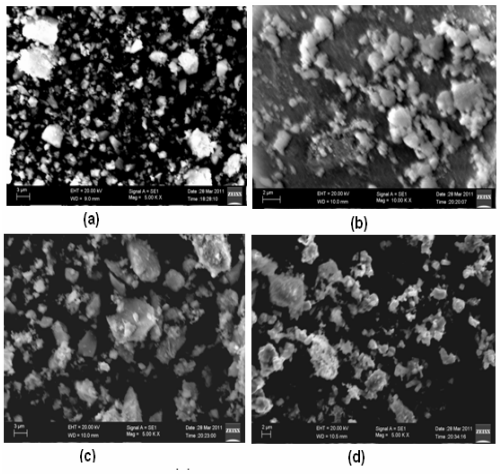


*Fig. 4. SEM images of nanoparticles of ZnS The particles are shown after synthesis (a) and after annealing at 300 $^0$C (b); and at 400 $^0$C (c); and at 600 $^0$C (d).*

The SEM images are presented in Fig. 4 as a function of annealing temperature. Fig. 4(a) shows the SEM image of as synthesized sample, the particles are in the nanometer size supporting the diffraction result. Annealing of particles at various temperature results in an agglomeration of particles as shown in Fig. 4. At higher annealing temperatures, the nanoparticles are seen merging with each other and forming a neck between the two particles.

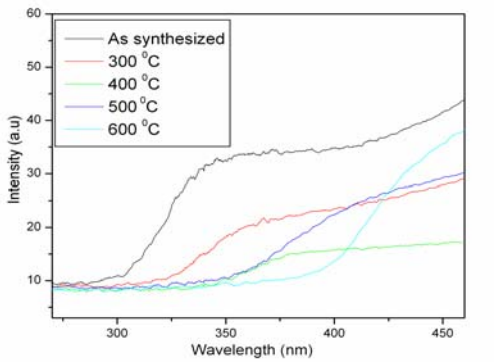


*Fig. 5. Reflectance spectra of as synthesized and annealed ZnS NCs.*

Fig. 5 shows diffuse reflectance spectra of as synthesized and annealed ZnS NCs. Reflectance of all annealed samples was decreased when compared to as synthesized sample. As the annealing temperature increases the absorption edge shifted towards longer wavelength side, which indicates that the band gap energy decreases as the annealing temperature increases. The band gap energy value of as prepared ZnS is 4 eV.

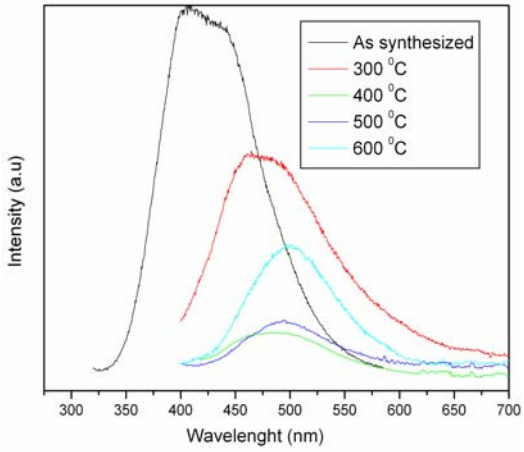


*Fig. 6. Room temperature Photoluminescence spectra of as synthesized and annealed ZnS NCs.*

Room temperature photoluminescence (PL) spectra of as prepared and annealed ZnS nanoparticles are shown in Fig. 6. For as prepared NCs overlapping of two PL peaks positioned at ~406 nm and ~ 430 nm was observed. These peaks can be attributed to sulfur vacancies and interstitial lattice defects. The trap levels with in the forbidden gap of chalcogenides due to sulfur vacancies may be of two types, internal sulfur vacancy and surface sulfur vacancy [25]. The surface sulfur vacancy state should be located closer to the conduction band than the internal sulfur vacancy state. Thus the peak observed at around ~406 nm can be attributed to the recombination of electrons at surface sulfur vacancy with the holes at the valance band, and the peak observed at ~430 nm can be attributed to internal sulfur vacancies. The broadening of PL peak can

be observed from figure and it can be attributed to size distribution.

Annealing up to 400 $^0$C causes the photoluminescence peak to shift from ~406 nm to ~496 nm with intensity quenching. The quenching of luminescence intensity can be attributed to the oxidation of sulfur into sulfate and elimination of lattice defects due to annealing. Red shift can be attributed to the quantum size effect. Annealing at 500 $^0$C, results in further small red shifted peak with small increase in intensity. This peak can be attributed to the presence of oxygen vacancies. The intensity of this peak increases with increasing annealing temperature to 600 $^0$C. The increase in intensity can be attributed to the increase in oxygen vacancies [26].

## 4. Conclusion

In summary, ZnS NCs was accomplished by chemical co-precipitation method. Structural, morphological and optical properties of ZnS NCs have been observed after heat treating. Hexagonal wurtzite phase of ZnS is attained by annealing ZnS NCs at 400 $^o$C, which is 600 $^o$C less compared to the bulk phase transition temperature of ZnS. In addition, ZnO NCs have been prepared simply by annealing ZnS in air at 600 $^o$C. Agglomeration of particles increased with increasing annealing temperature. Band gap energy of ZnS nanocrystals decreased with increasing annealing temperature. The present study also demonstrated the annealing temperature dependent quenching and raising behavior of photoluminescence emissions. These types of studies are useful while fabricating optoelectronic devices.

**Acknowledgements**

The authors are highly grateful to the University Grants Commission, New Delhi, India, for providing financial support.

## References

[1] Z. L. Wang, J. H. Song, Science. **312**, 242 (2006).
[2] A special issue on nanoscale materials, Acc. Chem. Res. **32**, 387 (1999).
[3] A special issue on nanostructured materials, Chem. Mater. **8**, 1569 (1996).
[4] L. Brus, Appl. Phys. A. **53**, 465 (1991).
[5] A. P. Alivisatos, Science. **271**, 933 (1996).
[6] D. J. Norris, M. G. Bawendi, Phys. Rev. B. **53**, 16338 (1996).
[7] D. J. Norris, A. L. Efros, M. Rosen, M. G. Bawendi, Phys. Rev. B. **53**, 16347 (1996).
[8] Prinsa Verma, A. C. Pandey, R. N. Bhargava, J. Optoelectron. Adv. Mater. **11**, 437 (2009).
[9] M. A. El-Sayed, Acc. Chem. Res. **37**, 326 (2004).
[10] N. Kumbhojkar, V. V. Nikesh, A. Khsirsagar, S. Mahamuni, J. Appl. Phys. **88**, 6260 (2000).
[11] S. B. Qadri, E. F. Skelton, D.Hsu, Dinsmore, A. D. Yang J, H. F. Gray, B. R. Ratna, Phys. Rev. B. **60**, 9191 (1999).
[12] S. H. Yu, M. Yoshimura, Adv. Mater.**14**, 296 (2002).
[13] W. Park, J. S. King, C. W. Neff, C. Liddell, C. J. Summers, Phys. Stat. Sol. **229**, 946 (2002).
[14] Zhi-Gang Chen, Lina Cheng, Hong-Yi Xu, Ji- Zi Liu, Jin Zou, Takashi Sekiguchi, Gao Qing (Max) Lu, Hui-Ming Cheng, Adv. Mater. **22**, 2376 (2010).
[15] G. Z. Shen, Y. Bando, D. Golberg, J. Phys. Chem. B. **110**, 20777 (2006).
[16] P. Hu, Y. Liu, L. Fu, L. Cao, D. Zhu, J. Phys. Chem. B. **108**, 936 (2004).
[17] D. Moore, Z. L. Wang, J. Mater. Chem. **16**, 3898 (2006).
[18] Michael W. Porambo, Anderson L. Marsh, Opt. Mater. **31**, 1631 (2009).
[19] Bhupendra B. Srivastava, Santanu Jana, Niladri S. Karan, Sayantan Paria, Nikhil R. Jana, D. D. Sarma, Narayan Pradhan, J. Phys. Chem. Lett. **1**, 1454 (2010).
[20] P. H. Borse, N. Deshmukh, R. F. Shinde, S. K. Date, S. K. Kulkarni, Mater. Sci. **34**, 6087 (1999).
[21] W. Q. Peng, G. W. Cong, S. C. Qu, Z. G. Wang, Opt. Mater. **29**, 313 (2006).
[22] C. S. Tiwary, P. Kumbhakar, A. K. Mitra, K. Chattopadhyay, J. Lumin. **129**, 1366 (2009).
[23] Changhyun Jin, Hyunsoo Kim, Kyungjoon Baek, Chongmu Lee, Mater. Sci. Eng. B. **170**, 143 (2010).
[24] T. Kuzuya, Y. Tai, S. Yamamuro, K. Sumiyana, Sci. Technol. Adv. Mater. **6**, 84 (2005).
[25] Hao Tang, Guoyue Xu, Luqian Weng, Lijia Pan, Ling Wang, Acta Mater. **52**, 1489 (2004).
[26] Hao-Ying Lu, Sheng-Yuan Chu, Soon-Seng Tan, J. Cryst. Growth**. 269**, 385 (2004).

*Corresponding author: vijayaraguru@gmail.com